Deformation of a stretched polymer knot

Yu-Jane Sheng,[1] Pik-Yin Lai,[2,*] and Heng-Kwong Tsao[3]
[1]*Department of Chemical Engineering, National Taiwan University, Taipei, Taiwan 107, Republic of China*
[2]*Department of Physics and Center for Complex Systems, National Central University, Chung-li, Taiwan 320, Republic of China*
[3]*Department of Chemical Engineering, National Central University, Chung-li, Taiwan 320, Republic of China*
(Received 26 July 1999)

The static properties of a knotted polymer under a stretching force f are studied by Monte Carlo simulations. Chain lengths up to $N=82$ and knot types of 0_1, 3_1, 4_1, 5_1, 6_1, and 8_1 are considered. Our simulation data show that the scaling laws proposed by de Gennes and Pincus for a single linear chain under traction force still hold for the knotted type polymers. That is, the average knot size under a force f scales as $\langle R_f \rangle \sim R_F^2 f$ at weak tension forces while for strong forces $\langle R_f \rangle \sim R_F^{1/\nu} f^{(1/\nu)-1}$, where $R_F \sim N^{\nu} p^{-4/15}$, $\nu \approx 3/5$ is the usual self-avoiding walk exponent and p is a topological invariant representing the aspect ratio (length to diameter) of a knotted polymer at its maximum inflated state. Our results also show that the elastic modulus of a knotted polymer is larger compared to an equal-length linear chain. More complex knots are in general stiffer. A simple composite spring model is employed to derive the increase in stiffness of knots relative to the linear chain, and the results agree well with the simulation data. Segregation of the crossings into a small tight region of the knot structure at strong forces is also observed.

PACS number(s): 61.41.+e, 83.10.Nn, 87.10.+e, 05.70.Fh

I. INTRODUCTION

The interest in studying knotted polymers originates from their important relation to biological systems. For example, DNA rings in bacteria take the form of a knotted ring, and there are certain types of enzymes that can act on circular DNA's and produce different types of DNA knots [1–3]. These proteins, RNA's, and DNA's are all polymers of biology origin. Thus investigations of knotted polymers can be of great help in understanding the behavior of ring DNA's. Our understanding of the static and dynamical properties of the physical knot system has progressed recently [4–7], despite the fact that great advances have been made in classifying knots and topological invariants in recent decades [8–11]. Some efforts have also been made to relate the topological invariants of knots to the static properties of the knotted polymers. Quake [4] developed a phenomenological model of the effects of knot complexity on static and dynamic properties in terms of the number of essential crossings, C. The theory has been tested against computer simulations, and agrees well with the radius of gyrations calculated. Grosberg *et al.* presented a mean field theory on the statistical mechanics of ring polymers [5], in which they introduced a topological invariant p which is the aspect ratio (length-to-diameter) of a knotted polymer at its maximum inflated state. The expression for the effects of topological complexity on the variation of static chain conformations (such as the radius of gyration) has been confirmed explicitly by our recent studies [7]. Stasiak *et al.* [12] performed experiments in testing the electrophoretic mobility of DNA knots in which a linear relation between average crossing numbers of knots and their speed of migration was observed. These results from theories, simulations, and experiments all indicate that it is possible to relate the behaviors of static and dynamic properties of different types of knotted polymers with rather simple topological invariants. It should be noted that this statement is not always correct. We have demonstrated that the nonequilibrium relaxation dynamics of a cut knotted polymer is found not to be in a simple relation with C or p only [7,13]. These results show that the local topological hindrance plays a crucial role in untying a knot through Brownian motions, and thus that knots should be classified into different groups based on their topological similarity and polynomial invariants [14].

The physical properties of many biological molecules, such as DNAs, are strongly affected by their topological properties. There have been some related theoretical studies on the elastic properties of linear DNA molecules associated with their double strand and helical structures [15–17], and also in terms of the topological linkage number [18]. Such theoretical work was motivated by recent advances in techniques with optical tweezers, which can manipulate DNA or protein molecules in a rather well controlled way and even artificially tie up a DNA molecule to form a knot [19], thus allowing the possibility to investigate many of the physical and even mathematical properties of knots experimentally. To probe topological effects on the static properties of knotted polymers is necessary in order to have a better understanding of their physical behavior. In this work, we extend our interest to a study of the deformations of knotted polymers under stretching forces. This situation is likely to be encountered in knot polymers undergoing gel electrophoresis, under shear flow, or being manipulated by optical tweezers. It is of great importance to study the mechanical or elastic responses of knotted molecules under external forces. There has been some recent *ab initio* calculation [20] on the breaking strength of a linear polyethylene chain with a trefoil knot in it (not a closed loop ring polymer); however, to our knowledge, there is as yet no theory or simulation results for the elastic properties of knots. Here we perform Monte Carlo simulations for knots under a constant stretching force, and

*Electronic address: pylai@spl1.phy.ncu.edu.tw

investigate how the force laws are modified by the topological properties of the knots. We also construct a simple theoretical model to analyze the increase in stiffness of the polymer due to the presence of knot structures. Since there are no experimental observations of this yet, our simulation results should be helpful in a study of ring polymer topology, and can also be compared with future experiments.

II. MODEL AND SIMULATION DETAILS

The polymer chain studied in this work is modeled as beads connected by stiff springs. The interactions between the nonbonded beads are through the square-well potentials,

$$U_{nb}=\begin{cases}\infty & (r<\sigma)\\ -\varepsilon & (\sigma\leqslant r<\lambda\sigma)\\ 0 & (\lambda\sigma\leqslant r),\end{cases} \tag{1}$$

where ε and σ are the energy and size parameters, respectively and $\lambda=1.5$. The monomeric ε and σ are units used for the reduced quantities for temperature and distances as $T^*=k_BT/\varepsilon$ and $R^*=R/\sigma$. The interactions between bonded beads are represented by a cutoff harmonic spring potential as

$$U_b=\frac{1}{2}k\sigma^2\left(\frac{r}{\sigma}-1.2\right)^2, \quad 1.0<\frac{r}{\sigma}\leqslant 1.4. \tag{2}$$

The potential is infinite elsewhere. We have chosen $k\sigma^2/\varepsilon=400$. The chain model is chosen to avoid bond crossing within the knotted chains. The system studied consists of a single closed ring polymer of N monomers ranging from 42 to 82. We study prime knot polymers of types 0_1, 3_1, 4_1, 5_1, 6_1, and 8_1. Prime knots are knots that cannot be factored into simpler knots, or in algebraic terms the polynomial invariant (such as Alexander or Jones polynomials) of a prime knot cannot be factorized into polynomials of simpler knots [11]. Figures 1(a), 1(b), and 1(c) (the left hand side parts) display knot diagrams of prime knots 0_1, 3_1, and 7_1 respectively. The simulations are performed under the conditions of constant temperature, volume, and total number of beads. In the present study, the reduced temperature $T^*=10$ is chosen so that the system is in a good solvent regime.

The initial configuration of the knot is generated by growing the chain bead by bead to the desired length on a cubic lattice. The subsequent motions of the chain is a continuum. The trial moves employed for chains are bead displacement motions [21], which involve randomly picking a bead and displacing it to a new position in the vicinity of the old position. The distance away from the original position is chosen with the probability that the condition of equal sampling of all points in the spherical shell surrounding the initial position must be satisfied. The new configurations resulting from this move are accepted according to the standard Metropolis acceptance criterion [22]. To simulate the stretching force in the $\pm z$ direction, the first bead is under an external potential $U=fz_1$, and the Mth ($M=N/2+1$) bead is under an external potential $U=-fz_M$, where z_1 and z_M are the coordinates of these two beads. Figure 1 shows the schematic representations of knots being stretched by force f. Runs for the same chain length at different stretching forces

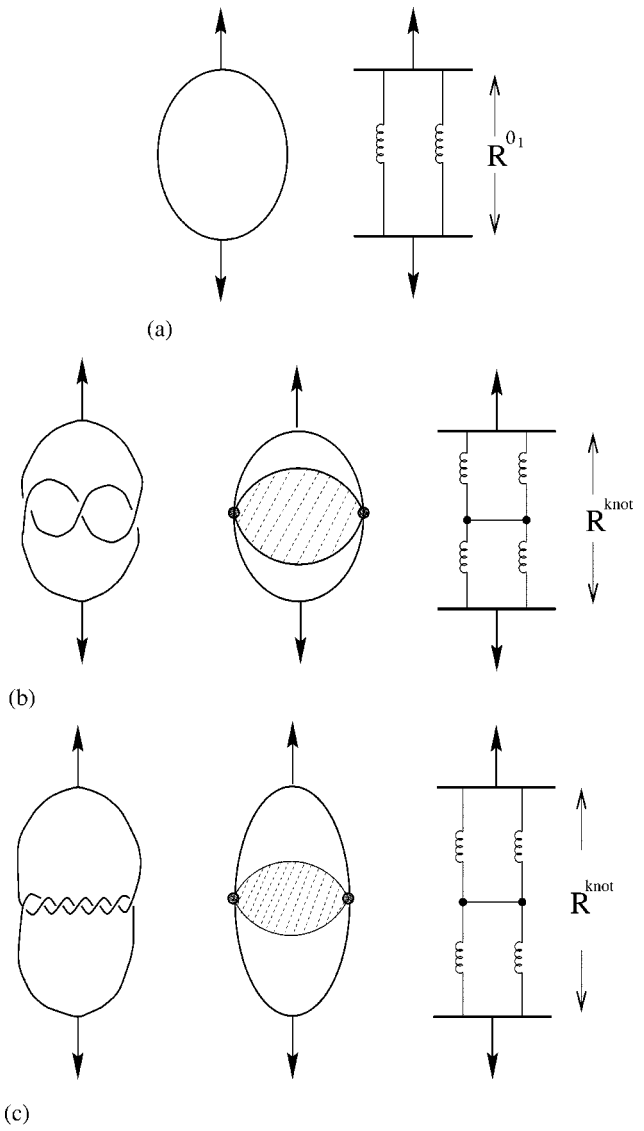

FIG. 1. Schematic representation of knots being stretched by the force f as composite spring systems. (a) Trivial knot 0_1. Left: circular trivial knot under tension. Right: system represented by a double spring system in parallel. (b) Trefoil 3_1. Left: picture of trefoil under tension. Middle: schematic representation as stretching of four strands, the crossing region is shaded. Right: composite spring representation, the center line is rigidly fixed to the two parallel strands. (c) Nontrivial knot under strong deformation, with the same notations as in (b).

are performed starting with the final configuration from a previous stretching force. All runs are equilibrated for several million steps. Measurements for static properties such as the knot size are taken over a period of 1–4 millions Monte Carlo steps/monomer. The equilibrium mean size parallel to the direction of the stretching force is then measured, which is given by

$$\langle R_f\rangle=\langle\sqrt{(x_M-x_1)^2+(y_M-y_1)^2+(z_M-z_1)^2}\rangle \tag{3}$$

where (x_1,y_1,z_1) are the coordinates of the first monomer in the chain and (x_M,y_M,z_M) are the coordinates of the $M^{th}=(N/2+1)^{th}$ monomer. The angular brackets $\langle\ \rangle$ denote ensemble average.

III. COMPOSITE SPRING MODEL FOR RING POLYMERS UNDER TENSION

Our aim is to derive the change in the stiffness, or the effective spring constants of a ring polymer, with or without knot, when it is stretched. Before we proceed, let us recall the well-known force laws in the case of a linear long flexible chain given by Pincus [23] and de Gennes [24]. According to Pincus [23], for a linear polymer chain of N monomers and monomer size a, under an external force f, the average end-to-end displacement, $\langle R_f \rangle$ along the force direction can be written in a scaling form as

$$\langle R_f \rangle = R_F \Phi(R_F/\xi), \tag{4}$$

where $R_F = aN^{\nu}$ is the Flory radius of the free linear chain, ξ is the tensile screening length [23,24], and $\Phi(x)$ is some dimensionless scaling function. ξ can be thought of as the blob size formed within the chain at temperature T under stretching force f with $f\xi = k_B T$. R_F and ξ are the two characteristic lengths of the system. In the limit of weak force, i.e. $R_F/\xi \ll 1$, R_f is expected to be linear in f. Therefore, the polymer has a Hooke's restoring force given by

$$\langle R_f \rangle \approx \frac{f}{k_B T} R_F^2 = aN^{2\nu}\mathcal{F}, \tag{5}$$

where the dimensionless reduced force $\mathcal{F} \equiv fa/(k_B T)$ is introduced for convenience. For the ideal case ($\nu = 1/2$), $\langle R_f \rangle$ is linear in N, which indicates that the tension force is transmitted along the backbone. However, in good solvents ($\nu \approx 3/5$), $\langle R_f \rangle$ is nonlinear in N at low forces for chains under traction. This is because the tension force is no longer transmitted along the backbone only, but also through interactions between certain pairs of monomers. We believe this effect will manifest itself in knotted type polymers, since they are usually more compact than their equal-length counterparts.

For a chain under a stronger external force, that is, $R_F/\xi \gg 1$, $\Phi(x)$ is assumed to be proportional to x^b, where b can be determined by the condition $\langle R_f \rangle \sim N$. Thus the end-to-end extension can be estimated to be

$$\langle R_f \rangle \approx R_F^{1/\nu} \left(\frac{f}{k_B T} \right)^{(1/\nu)-1} = aN\mathcal{F}^{1/\nu - 1}. \tag{6}$$

In good solvents, where $\nu \approx 3/5$, $\langle R_f \rangle \propto f^{2/3}$, instead of the linear Hooke's law. We expect that these scaling laws will also hold for knotted type ring polymers with sufficient length, i.e., far from the tight knot limit. However, for the knotted chains, extra interactions will emerge, and they are mainly from the topological constraints imposed upon the chains.

Now consider the simplest ring polymer, the trivial knot 0_1, which also consists of N monomers. Let the stretching forces act on the first and $(N/2+1)$th monomers as in our simulation. It is obvious that this circular chain will be stiffer than the linear chain of the same length, simply because there are two strands to balance the same f. One can schematically represent the trivial knot under tension as the spring system depicted in Fig. 1(a). Simple calculation gives the size of the 0_1 knot under a stretching force f as

$$R^{0_1} = a\left(\frac{N}{2}\right)^{2\nu} \frac{\mathcal{F}}{2} = \frac{1}{2^{1+2\nu}} R_f^{linear} \tag{7}$$

in the weak force regime, where R_f^{linear} is the size of a linear chain of N monomers under the tension f as given in Eq. (5). For the ideal $\nu = 1/2$ case, the extension is four times less than that of a linear chain, which can be easily understood: there are two springs of twice the stiffness (length of each strand is halved). For stronger forces, a similar calculation using the Pincus law for the springs gives

$$R^{0_1} = \frac{1}{2^{1/\nu}} R_f^{linear} \tag{8}$$

in the Pincus regime.

For the case of nontrivial prime knots, such as 3_1, 4_1, etc., the situation is more complicated; nevertheless one can still proceed for a rough estimation. Under the action of the stretching force, one expects the crossings will be more or less concentrated around the middle portion of the knot, as depicted schematically in Fig. 1(b). In the weak force regime, the knot is not strongly deformed, the portion of segments spend in the crossing region is comparable to those in the noncrossing regions [the middle of Fig. 1(b)]. Thus, on average, there are roughly $N/4$ monomers on each side of the noncrossing regions. Again view the system as a composite spring system as shown, with the crossing region represented schematically by a rigid line connecting the two strands, one can estimate the size of the knot to be

$$R^{knot} \approx 2a\left(\frac{N}{8}\right)^{2\nu} \frac{\mathcal{F}}{2} = \frac{1}{2^{6\nu}} R_f^{linear}. \tag{9}$$

For the strong deformation Pincus regime, the crossings are more tightly located in a smaller crossing region [see Fig. 1(c)], and hence the average portion of segments spend in the crossing region would be fewer and more sensitive to the value of C of the knot. One can estimate a lower bound of its size by a similar calculation as above [Fig. 1(b)]; however, using the Pincus force law, one obtains

$$R^{knot} > \frac{1}{2^{1+1/\nu}} R_f^{linear}. \tag{10}$$

In order to obtain an order of magnitude estimate, one can make a bold assumption that about 1/3 of segments are in the crossing region on average as schematically depicted in the middle of Fig. 1(c), then one obtains

$$R^{knot} \sim \frac{1}{3} \frac{1}{2^{1/\nu - 1}} R_f^{linear}. \tag{11}$$

Using the best known value of the self-avoiding walk exponent [25] $\nu \simeq 0.588$ for polymers in good solvent conditions, these predictions will be compared with our simulation data in Sec. IV.

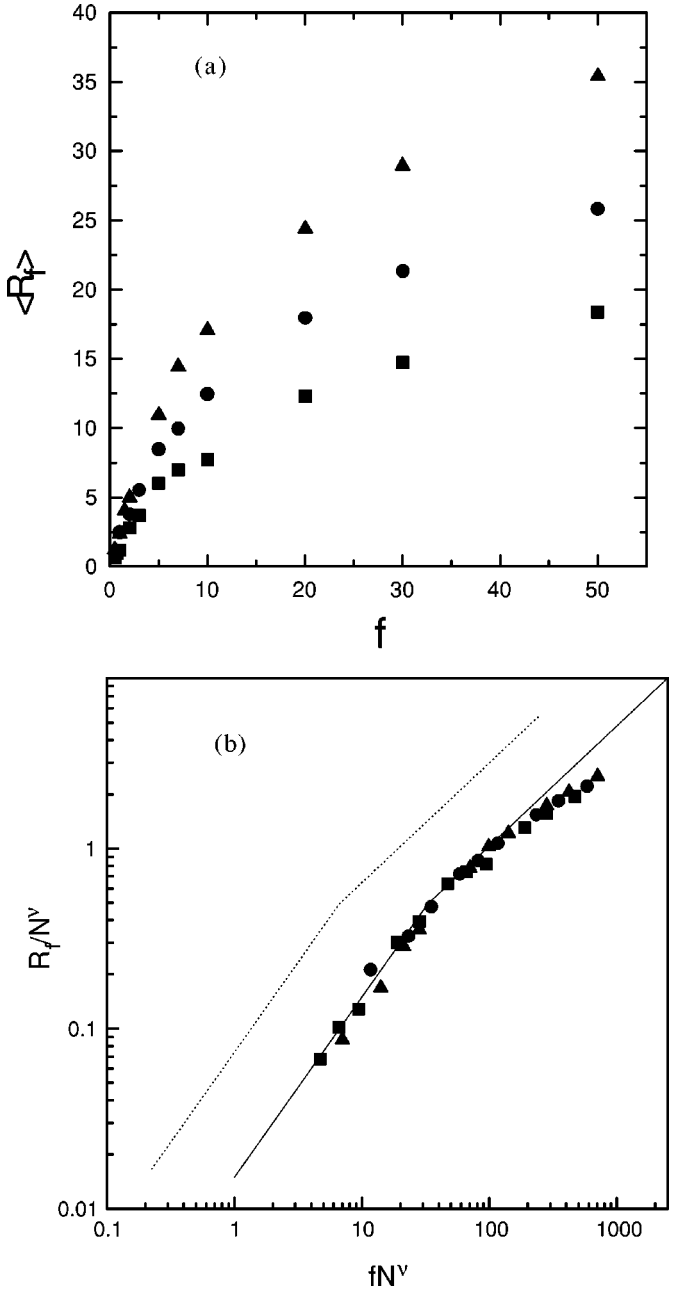

FIG. 2. (a) Mean size of knot polymer (in unit of σ) vs the stretching force (in unit of k_BT/σ) for the 0_1 trivial knot at various chain lengths: (■) $N=42$, (●) $N=60$, and (▲) $N=82$. (b) Same data as in (a) but plotted with R_f/N^ν vs fN^ν. Solid lines are slopes of 1 and 2/3 from Eqs. (5) and (6). Scaling curves for the linear chain are denoted by the dotted lines which have the same slopes as the solid lines.

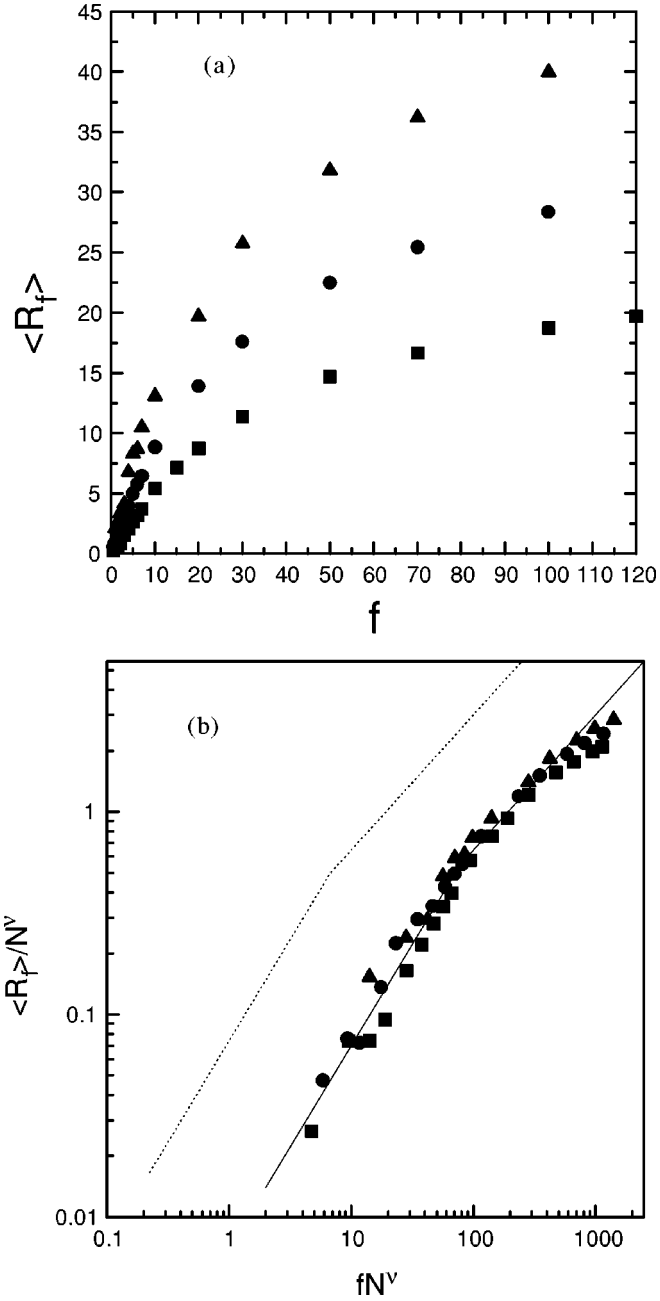

FIG. 3. (a) Mean knot size (in unit of σ) vs the stretching force (in unit of k_BT/σ) for the 3_1 knot at various chain lengths: (■) $N=42$, (●) $N=60$, and (▲) $N=82$. (b) Same data as in (a) but plotted with $\langle R_f\rangle/N^\nu$ vs fN^ν. Solid and dotted lines have the same meaning as in Fig. 2.

IV. RESULTS AND DISCUSSIONS

We have performed Monte Carlo simulations to investigate the dependence of the average knot size on the stretching force for the knotted polymers. Figure 2(a) shows the variation of $\langle R_f\rangle$ versus f for the trivial circular knot (0_1) at different chain lengths. Since they are of the same type of knots, the topological effect must be similar. Thus we expect their sizes will obey the same scaling laws as the linear chain does. In Fig. 2(b) the scaled mean size $\langle R_f\rangle/N^\nu$ is plotted as a function of fN^ν for various chain lengths. The deformation of the chain obeys the linear Hooke's law in the weak force regime, and displays a Pincus scaling behavior in the strong force regime. As in the case of a linear chain, the knot with the longer chain length reaches the scaling law at weaker forces [21]. The scaling curve for the linear chain is also shown for comparison. Note that it can clearly be seen that the entire scaling curve for the knotted polymers has shifted to the stronger force region, i.e. the knotted polymers are more resistant to external forces than the linear polymers. In the weak deformation regime, our data indicate that the size of the circular polymer is about 4.5 times less as compared to the linear polymer under the same force and with the same

TABLE I. Comparison of the composite spring model predictions with the simulation data for the increase in stiffness relative to the linear chain of the same length. $\nu=0.588$ is used in the theoretical results.

	Linear regime		Pincus regime	
Knot	Theory	Data	Theory	Data
0_1	$2^{1+2\nu}\approx 4.52$	4.6 ± 0.4	$2^{1/\nu}\approx 3.25$	3.1 ± 0.3
3_1	$2^{6\nu}\approx 11.54$	11.0 ± 0.6	$3\times 2^{1/\nu-1}\approx 4.88$	4.7 ± 0.3

number of monomers. This is in good agreement with our prediction using the composite spring model in Eq. (7) with $2^{1+2\nu}\simeq 4.6$. In the strong deformation Pincus regime, the increase in stiffness is less, our data give about a factor of 3.1 increase which also agrees well with the predicted value of $2^{1/\nu}\simeq 3.25$ in Eq. (8). No universal scaling law applies for the very strong force regime, and the deformation behavior becomes model dependent as significant bond stretching occurs in this regime.

Trefoils of different lengths under stretch is also investigated. Figure 3(a) shows the $\langle R_f\rangle$ versus f for the 3_1 knot at different chain lengths. The scaled mean size $\langle R_f\rangle/N^{\nu}$ is plotted as a function of fN^{ν} for various chain lengths as shown in Fig. 3(b). Again the deformation of the chain obeys Hooke's law and the Pincus force law in the weak and strong force regimes, respectively. The scaling curve for the knotted polymers shifts even further into the stronger force region relative to the linear chain. This suggests that the more complex knot is more resistant to external forces for knots of the same lengths. In the weak deformation regime, the size of the trefoil is about 11.5 times less than that of the linear chain, which is close to the predicted value of $2^{6\nu}\approx 11.54$ from Eq. (9). In the strong deformation regime, the size is about five time less, which is consistent with the upper bound of $2^{1+1/\nu}\approx 6.4$ from Eq. (10), and even agrees reasonably well with the crude estimation of $3\times 2^{1/\nu-1}\approx 4.88$ from Eq. (11). These results are summarized in Table I.

To study the topological effects of different knot types, we performed simulations for various prime knots with the same length ($N=60$). As shown by Grosberg *et al.* [5], the topological invariant p, given by the ratio of the contour length to the diameter of the knot in its maximally inflated state, is a good quantity to characterize the complexity of a knot. The maximally inflated state of a knot is achieved by imagining that the polymer knot is made of a balloon tube, which is then blown up maximally such that the different segments of the balloon are touching each other. p is then the ratio of the contour length of the inflated balloon tube to its diameter. The values of p were calculated by Monte Carlo simulations by Katritch *et al.* [6] for various prime knots, and these values of p will be used in the present study. Data in Fig. 4(a) indicate that the deformation decreases as the complexity in knots increases for the same stretching force f. This again indicates that the elastic modulus of a less complex knot is less, and will be more susceptible to external forces. In Fig. 4(b) the scaled mean knot size $\langle R_f\rangle/p^{-4/15}$ is plotted as a function of $fp^{-4/15}$ for various types of knotted polymers. Though the data are somewhat scattered in the weak force region, they seem to obey the linear scaling rule approximately. The width of the crossover regime between

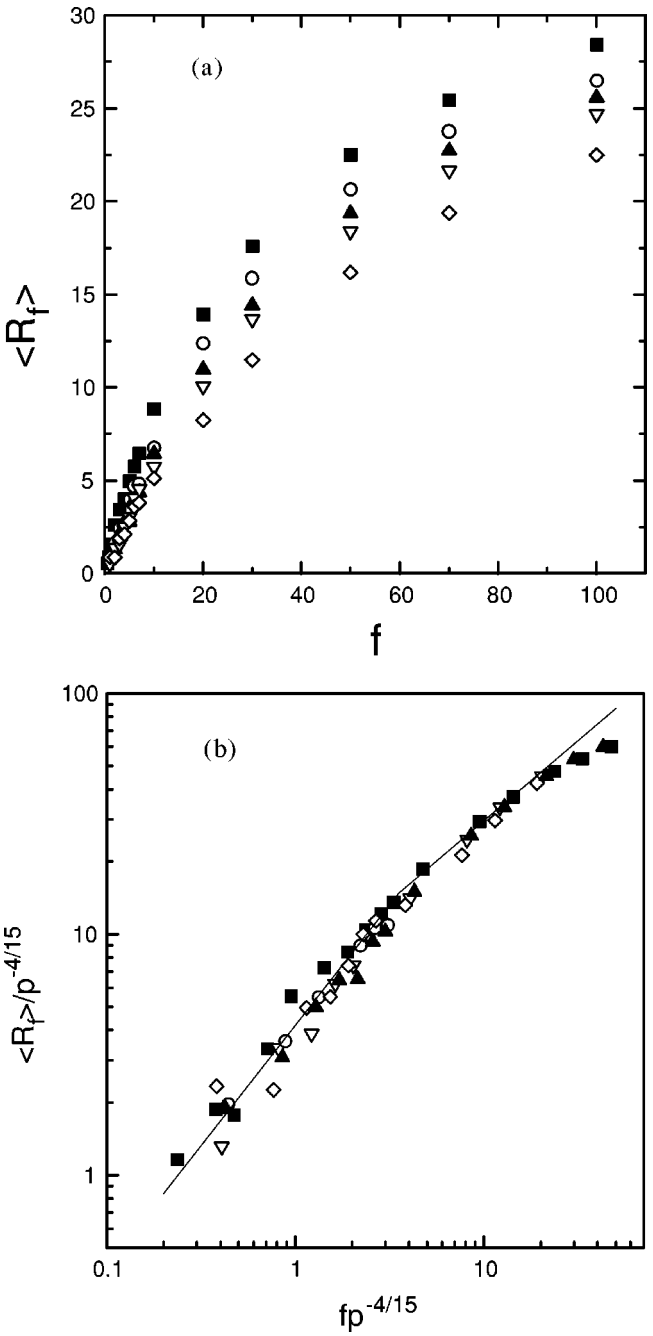

FIG. 4. (a) Mean knot size (in unit of σ) vs the stretching force (in unit of k_BT/σ) for different types of knots at the same chain length ($N=60$): (■) 3_1, (○) 4_1, (▲) 5_1, (▽) 6_1, and (◇) 8_1. (b) Same data as in (a) but plotted with R_f/p^{α} vs fp^{α}, where $\alpha=-4/15$. Solid lines are slopes of 1 and 2/3.

linear and Pincus behavior is fairly narrow, as in the case of the linear chain [21]. For strong forces, the Pincus scaling rule applies and the elastic response is more nonlinear.

To investigate the effect of distinct knot types on the elastic response, other prime knots of types 4_1, 5_1, 6_1, and 8_1 are also simulated. As in the case of a linear flexible polymer chain, we propose that the global equilibrium elastic properties of a knot depend on the global shape deformation relative to the dimension of the knot under no external force. We denote the free Flory radius of the knot under no force by R_F; there have been scaling results [4,5] for R_F in terms of

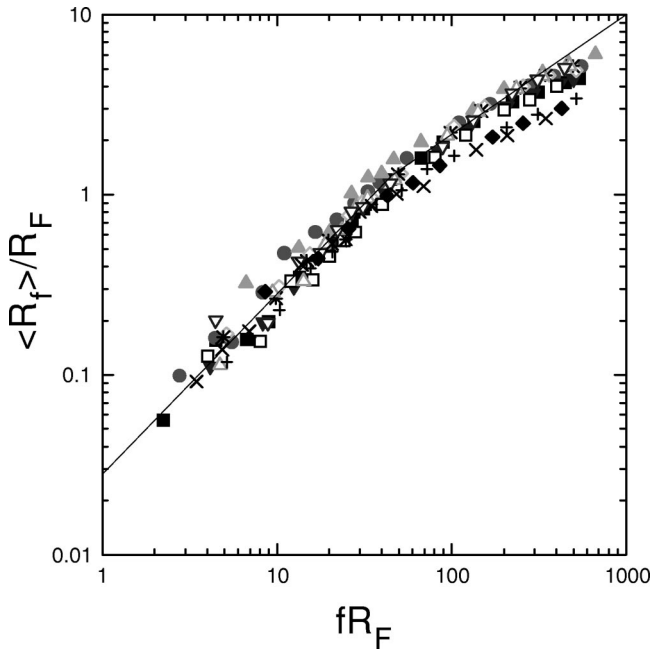

FIG. 5. Scaled knot size ($\langle R_f \rangle / R_F$) vs the scaled stretching force fR_F (in unit of k_BT) for different types of knots at various chain lengths. $R_F \sim N^{\nu} p^{-4/15}$. Symbols: (+) 0_1, $N=42$, (×) 0_1, $N=60$; (filled ◇) 0_1, $N=82$; (■) 3_1, $N=42$; (●) 3_1, $N=60$; (▲) 3_1, $N=82$; (▼) 4_1, $N=42$; (◇) 4_1, $N=60$; (□) 5_1, $N=42$; (*) 5_1, $N=60$; (△) 6_1, $N=60$; (▽) 8_1, $N=60$.

the topological invariants that characterize the complexity of the knot. As shown by Grosberg *et al.* [5] and verified by our previous simulation [7], $R_F \sim N^{\nu} p^{-4/15}$. Thus the mean knot size is proposed to have the same scaling form as given by Eq. (4) with the corresponding linear and Pincus regimes given by Eqs. (5) and (6) respectively. Figure 5 shows the scaled mean size in unit of the free Flory radius of the knot under no force ($\langle R_f \rangle / R_F$) vs the scaled stretching force (fR_F) for different types of knots at various chain lengths. As we can see, the data scale reasonably well. The scaling relations of the linear chains also hold for knotted type polymers, as long as a correct scaling relation for the free radius of knotted polymers is defined. The result is consistent with previous studies, in that the topological effects of the knotted structures on the static properties can be accounted for with a rather simple relation of their topological invariants [7].

Figures 6(a) and 6(b) are snapshots of the equilibrium conformations for 3_1 and 8_1 knots stretched with six different values of forces. The deformations of the 3_1 knot are obviously stronger than that of the 8_1 knot under the same force. Note that at weak force regimes, the distributions of the crossings are quite uniform; however, as forces increase, the crossings tend to segregate to a small region. The segregation region can move up and down within the knot due to Brownian motions. At a very strong force, the crossings become very tight and stay in a certain part of the knot. To give an idea of the generic picture of the conformations of the knots at various regimes of tension, one can compare the values of f in Fig. 6 with the simulation data, such as those shown in Fig. 3. For the 3_1 knots in Fig. 6(a), the conformations at $f=1$ and 4 lie in the linear regime; those at $f=10$ and 20 are in the Pincus regime, while the last two conformations are in the strongly stretched model dependent re-

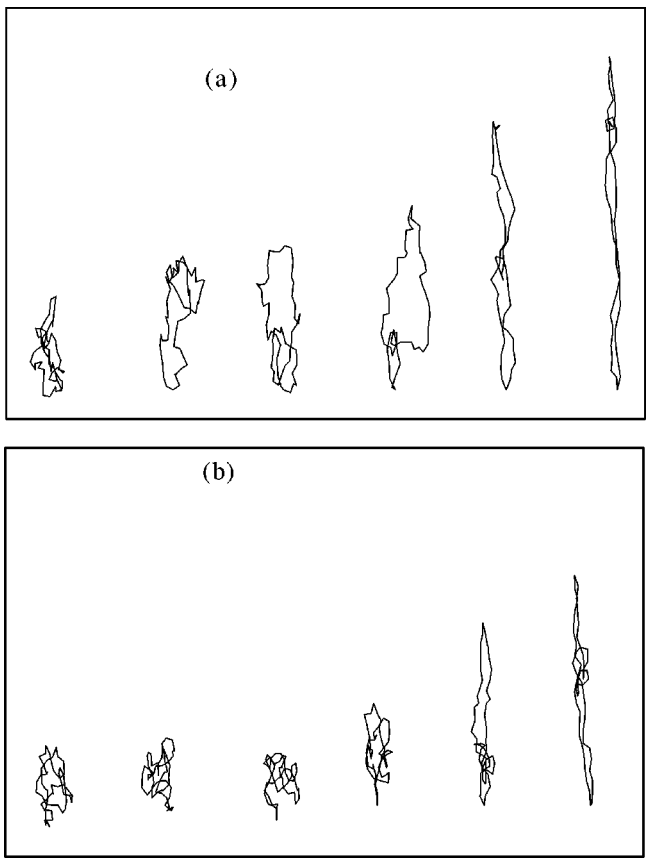

FIG. 6. The snapshots of the equilibrium conformations for knots of $N=60$ being stretched at scaled force $f\sigma/(k_BT) = 1,\ 4,\ 10,\ 20,\ 50$, and 100. (a) 3_1 knot; the six configurations for increasing f correspond to the regimes as follows: linear, linear, Pincus, Pincus, model dependent, and model dependent, respectively. (b) 8_1 knot; configurations correspond to linear, linear, linear, Pincus, Pincus, and model dependent regimes for increasing f.

gime. For the 8_1 knot in Fig. 6(b), the first three configurations are in the linear regime, followed by two conformations in the Pincus regime and a final one in the model dependent regime. As expected, a more complex knot is less deformed under the same force. This can be understood intuitively as follows: in the absence of an external force, knots with more essential crossings will have more segments spending time in the crossing region [see the middle of Fig. 1(b)]. As an external stretching force is applied to deform the knot, it has to overcome a stronger effective ''friction'' or hindrance for the more complex knot, and hence more complex knots are stiffer.

V. CONCLUDING REMARKS

In this work, we have performed Monte Carlo simulations to investigate the static behaviors of knotted polymers under a stretching force in good solvents. The polymers were simulated in a continuous space using a bead-spring chain model. The nonbonded interactions are square-well potentials, and the bonded beads interact through a cutoff harmonic spring potential. The chain model is chosen to avoid a bond crossing within the knotted chains. Chain lengths from $N=42$ to 82 and prime knots of 0_1, 3_1, 4_1, 5_1, 6_1, and 8_1 are considered. Our Monte Carlo results for the static quantity veri-

fied the fact that the scaling laws proposed by de Gennes and Pincus for linear chains under traction force also hold for knotted type polymers. That is, the elastic response depends only on the relative deviation of the knot from its undeformed dimension, and a scaling law in the form of Eq. (4) holds. In particular, the knot size scales as $\langle R_f \rangle \sim R_F^2 f$ at weak tension forces, and as $\langle R_f \rangle \sim R_F^{1/\nu} f^{(1/\nu)-1}$ for strong forces with $R_F \sim N^{\nu} p^{-4/15}$. One expects these scaling results would be valid as long as the knot is far from the tight knot limit, or provided that the chain is long enough so that universal scaling results apply. On the other hand, significant bond stretching occurs under extremely strong forces or when the knot is tight; the elastic response depends on the particular interaction potential between the monomers, and hence the deformation behavior becomes model-dependent and no universal scaling laws apply. Furthermore, our results show that for the same number of beads, all scaling curves of knotted polymers shift to a stronger force region. This means that the elastic modulus of a knotted polymer is larger as compared to a linear chain of the same length. Based on a simple model that represents the knot by a composite spring system, a decrease in the sizes of trivial and nontrivial knots was derived. Although the model is crude and could not even distinguish different nontrivial knots, its prediction agrees very well quantitatively for the trivial knot. Even for the nontrivial trefoil, this simple model still gives reasonable predictions when compared to the simulation data. For knotted polymers of the same length, the deformation decreases as the complexity of the knots increases at the same stretching force. More complex knots are stiffer. We have also observed that at very strong forces, the crossings tend to segregate into a small region of the knot structure. We hope our results can stimulate further experimental and theoretical studies on knotted molecules.

ACKNOWLEDGMENTS

This research was supported by the National Council of Science of Taiwan under Grant Nos. NSC 89-2118-M-008-003 and 88-2218-E-002-046. Computing time provided by the Simulational Physics Lab., National Central University is gratefully acknowledged.

[1] W. R. Bauer, F. H. C. Crick, and J. H. White, Sci. Am. **243**, 118 (1980).
[2] N. R. Cozzarelli, S. J. Spengler, and A. Stasiak, Cell **42**, 325 (1985).
[3] S. A. Wasserman and N. R. Cozzarelli, Science **232**, 951 (1986).
[4] S. R. Quake, Phys. Rev. Lett. **73**, 3317 (1994).
[5] A. Yu. Grosberg, A. Feigel, and Y. Rabin, Phys. Rev. E **54**, 6618 (1996).
[6] V. Katritch, J. Bednar, D. Michoud, R. G. Scharein, J. Dubochet, and A. Stasiak, Nature (London) **384**, 142 (1996).
[7] Y.-J. Sheng, P.-Y. Lai, and H.-K. Tsao, Phys. Rev. E **58**, R1222 (1998).
[8] V. F. R. Jones, Bull. Am. Math. Soc. **12**, 103 (1985).
[9] F. Y. Wu, Rev. Mod. Phys. **64**, 1099 (1992).
[10] L. H. Kauffman, *Knots and Physics*, 2nd ed. (World Scientific, Singapore, 1993).
[11] G. Burde and H. Zieschang, *Knots* (de Gruyter, Berlin, 1985).
[12] A. Stasiak, V. Katritch, J. Bednar, D. Michoud, and J. Dubochet, Nature (London) **384**, 122 (1996).
[13] P.-Y. Lai, Y.-J. Sheng, and H.-K. Tsao, Physica A (to be published).
[14] P.-Y. Lai, Y.-J. Sheng, and H.-K. Tsao (unpublished).
[15] J. F. Marko and E. D. Siggia, Macromolecules **28**, 8759 (1994).
[16] J. F. Marko and E. D. Siggia, Science **256**, 506 (1994); Phys. Rev. E **52**, 2912 (1995).
[17] H. Zhou, Y. Zhang, and Z.-C. Ou-Yang, Phys. Rev. Lett. **82**, 4560 (1999).
[18] J. F. Marko, Phys. Rev. E **59**, 900 (1999).
[19] Y. Arai, R. Yasuda, K.-I. Akashi, Y. Harada, H. Miyata, K. Kinoshita, Jr., and H. Itoh, Nature (London) **399**, 446 (1999).
[20] A. M. Saitta, P. D. Soper, E. Wasserman, and M. L. Klein, Nature (London) **399**, 46 (1999).
[21] Y.-J. Sheng, P.-Y. Lai, and H.-K. Tsao, Phys. Rev. E **56**, 1900 (1997).
[22] M. P. Allen and D. J. Tildesley, *Computer Simulations of Liquids* (Oxford University Press, New York, 1987).
[23] P. Pincus, Macromolecules **9**, 386 (1976).
[24] P. G. de Gennes, *Scaling Concepts in Polymer Physics* (Cornell University Press, Ithaca, NY, 1979).
[25] J. C. Le. Guillou and J. Zinn-Justin, Phys. Rev. Lett. **39**, 95 (1977); Phys. Rev. B **21**, 3976 (1980).